



HAL
open science

Influence of the processing parameters of slurries for the deposit of nickelate thick films

S. Castillo, R.F. Cienfuegos, M.L. Fontaine, P. Lenormand, Patrice Bacchin,
Florence Ansart

► To cite this version:

S. Castillo, R.F. Cienfuegos, M.L. Fontaine, P. Lenormand, Patrice Bacchin, et al.. Influence of the processing parameters of slurries for the deposit of nickelate thick films. *Materials Research Bulletin*, 2007, 42 (12), pp.2125-2131. 10.1016/j.materresbull.2007.01.011 . hal-00201545

HAL Id: hal-00201545

<https://hal.science/hal-00201545>

Submitted on 1 Mar 2022

HAL is a multi-disciplinary open access archive for the deposit and dissemination of scientific research documents, whether they are published or not. The documents may come from teaching and research institutions in France or abroad, or from public or private research centers.

L'archive ouverte pluridisciplinaire **HAL**, est destinée au dépôt et à la diffusion de documents scientifiques de niveau recherche, publiés ou non, émanant des établissements d'enseignement et de recherche français ou étrangers, des laboratoires publics ou privés.



Open Archive Toulouse Archive Ouverte (OATAO)

OATAO is an open access repository that collects the work of Toulouse researchers and makes it freely available over the web where possible.

This is an author-deposited version published in: <http://oatao.univ-toulouse.fr/>
Eprints ID : 2454

To link to this article :

URL : <http://dx.doi.org/10.1016/j.materresbull.2007.01.011>

To cite this version : Castillo, Simone and Cienfuegos, R. F. and Fontaine, Marie-Laure and Lenormand, Pascal and Bacchin, Patrice and Ansart, Florence (2007) [*Influence of the processing parameters of slurries for the deposit of nickelate thick films.*](#) Materials Research Bulletin, vol. 42 (n° 12). pp. 2125-2131. ISSN 0025-5408

Any correspondence concerning this service should be sent to the repository administrator: staff-oatao@inp-toulouse.fr

Influence of the processing parameters of slurries for the deposit of nickelate thick films

S. Castillo ^{a,*}, R.F. Cienfuegos ^a, M.L. Fontaine ^b, P. Lenormand ^a,
P. Bacchin ^c, F. Ansart ^a

^a CIRIMAT Laboratory, UMR CNRS 5085, Paul Sabatier University, 118 route de Narbonne, 31062 Toulouse cedex 4, France

^b SINTEF, Pb. 124 Blindern, NO-0314 Oslo, Norway

^c LGC UMR CNRS 5503, Paul Sabatier University, 118 route de Narbonne, 31062 Toulouse cedex 4, France

Abstract

Thick films cathodes for Solid Oxide Fuel Cells (SOFC) are prepared by dip-coating slurries made of several lanthanum nickelate oxide powders onto yttria stabilized zirconia (YSZ) substrates. The processing parameters for the slurries preparation and the multilayers coating have been optimized to obtain homogeneous, crack-free, thick and adherent films after heat treatment.

Keywords: A. Multilayers; A. Oxides; B. Sol-gel chemistry; C. Electron microscopy; D. Microstructure

1. Introduction

The development of new conversion energy systems like Solid Oxide Fuel Cells (SOFC) requires to drastically decrease their working temperature from 1000 °C to 700 °C in order to reduce their manufacturing costs and to optimize materials lifetime. In such systems, the cathode preferentially consists of a MIEC active material (mixed ionic and electronic conductor) coated onto an oxygen ionic conducting electrolyte, which is commonly yttria stabilized zirconia (YSZ) [1–5]. Use of MIEC allows to not limit the oxygen reduction to occur at the triple phase boundaries region. An other way to improve the electrochemical performances of the cathode is to increase the amount of active material by the deposition of porous films with high effective surface area. In this work, these two approaches have been combined. Cathode materials were two Ruddlesden-Popper phases, such as $\text{La}_2\text{NiO}_{4+\delta}$ and $\text{La}_4\text{Ni}_3\text{O}_{10}$. Previous work showed that the ratio La/Ni influences the cathode conductivity [4,6]. Therefore, cathodes with different La/Ni ratio have been prepared as monophasic multilayers and graded multilayers. To control the effective surface area of the cathode, a processing method based on the suspension deposition technique [7,8] was developed to prepare thick cathodes with graded compositions.

Within this process, the first objective was the obtention of stable suspensions. These suspensions were prepared from the dispersion of lanthanum nickelates crystallites ($\text{La}_2\text{NiO}_{4+\delta}$ and $\text{La}_4\text{Ni}_3\text{O}_{10}$) [9,10] synthesized by a sol-gel route, in a solution made of a solvent, a dispersant and some organic additives [11,12]. The stability of the suspensions

* Corresponding author. Tel.: +33 5 61 55 61 09; fax: +33 5 61 55 61 63.

E-mail address: castillo@chimie.ups-tlse.fr (S. Castillo).

was achieved by adjusting the dispersant concentration [12]. The stable slurries were then used to coat thick cathodic layers onto YSZ electrolyte, using the dip-coating technique and a controlled withdrawal speed [13].

The second objective was the preparation of different cathodic architectures by depositing several layers of $\text{La}_2\text{NiO}_{4+\delta}$ and $\text{La}_4\text{Ni}_3\text{O}_{10}$ materials onto YSZ electrolyte. In some cases, the suspensions were also deposited onto a thin cathodic interlayer obtained by dip-coating in a polymeric sol of $\text{La}_2\text{NiO}_{4+\delta}$ or $\text{La}_4\text{Ni}_3\text{O}_{10}$ precursors [5]. This duplex microstructure design is expected to enhance the cathode performances due to a more intimate cathode/electrolyte interface [6,14]. The microstructure of different architectures was investigated by field emission gun scanning electron microscopy (FEG-SEM) and X-ray diffraction (XRD).

2. Experimental procedure

The raw material, in the form of fine powder, was prepared by a derived sol-gel method [2]. The flow chart of the powders preparation is reported in Fig. 1. The powders were characterized by X-ray diffraction (BRUKER axs D4 ENDEAVOR diffractometer), thermal analysis (SETARAM TGA 92), Zeta potential and granulometry (Zetasizer 300HS, Malvern Instruments Ltd.), Scanning Electron Microscopy (SEM) (JEOL-6700F) to determine the morphology of the particles after calcination.

The crystallized powders were dispersed into an azeotropic mixture of methylethylketone (MEK) and ethanol (ETOH) also containing a commercial dispersant C213 and two additives such as PVB binder and phthalate plasticizer to achieve adequate viscosity and cohesion in the slurries [10,12]. A 3 min ultrasonic step (SinapTec Power Unit NEXUS 198) was required to obtain an homogeneous slurry. The composition of the slurries prepared with different amounts of dispersant is reported in Table 1.

The slurries were characterized by thermogravimetric and thermodifferential analyses in air, during heating with a rate of 5 K/min from 150 °C to 1000 °C (preliminary evaporation of solvent at 150 °C was achieved in a drying oven in order to obtain dried mixture). The size and the charge of aggregates were obtained by Zeta potential and granulometry measurements, respectively, in diluted MEK/ETOH solutions (0.1 mg/mL). The best compositions for preparing stable slurries were chosen from these experiments.

The films were dip-coated according to the following procedure: YSZ substrates were immersed into the slurry and withdrawn at a controlled speed (3 cm/min). In order to avoid cracks during annealing, the heating treatment of the monolayer was defined according to the thermal decomposition profile of the slurry. Thick layers were obtained by

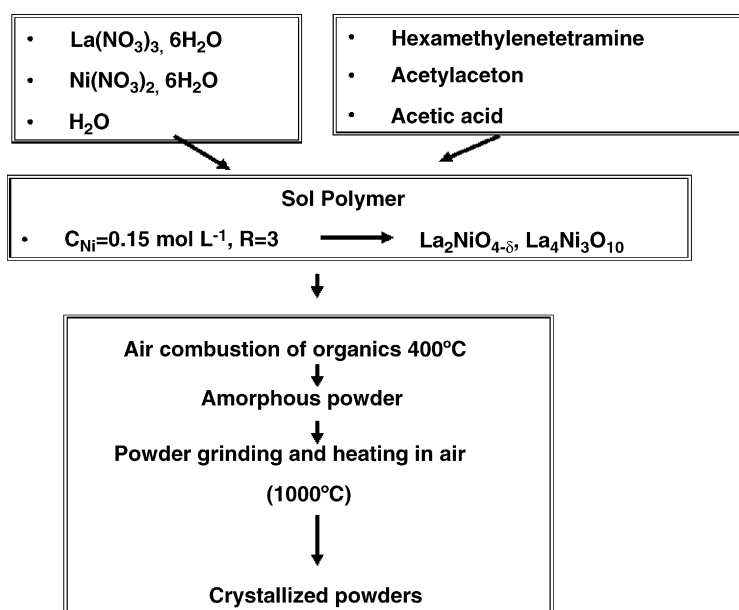


Fig. 1. Flow chart of powder preparation.

Table 1
Slurry composition

Composition	(1)	(2)	(3)
	g	g	g
Powder ($\text{La}_2\text{NiO}_{4+\delta}$ or $\text{La}_4\text{Ni}_3\text{O}_{10}$)	1.00	1.00	1.00
Solvent (MEK/ETOH)	1.00	1.00	1.00
Dispersant (C213)	0.02	0.04	0.06
Binder (poly vinyl butyral, PVB)	0.12	0.12	0.12
Plasticizer (dioctyl phthalate)	0.02	0.02	0.02

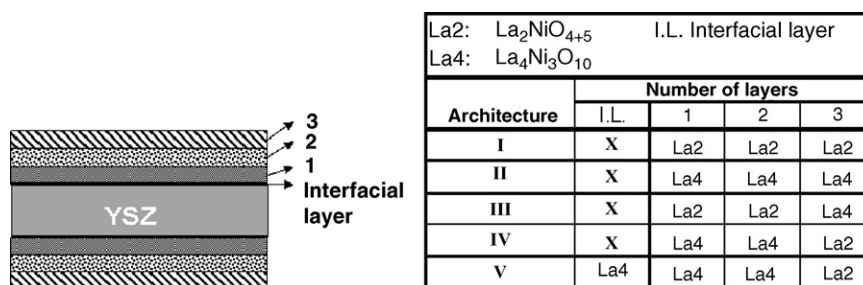


Fig. 2. Layer array.

repeating the dip-coating and thermal treatment steps. After three deposits, various cathode architectures were prepared as illustrated in Fig. 2.

One architecture was also built on a cathodic interlayer obtained by dip-coating YSZ electrolyte in a precursor lanthanum nickelate oxide sol, heated slowly up to 700 °C (50 °C/h), then annealed at 1000 °C for 2 h with an heating rate of 100 °C/h [5].

The cathodes thickness was measured by optical interferometry (Dektak 3030 ST).

3. Results and discussion

The powders were obtained as single phases of $\text{La}_2\text{NiO}_{4+\delta}$ and $\text{La}_4\text{Ni}_3\text{O}_{10}$ oxides. The corresponding patterns are reported in Fig. 3 and are in good agreement with literature data [3,9]. The crystallite sizes were calculated from

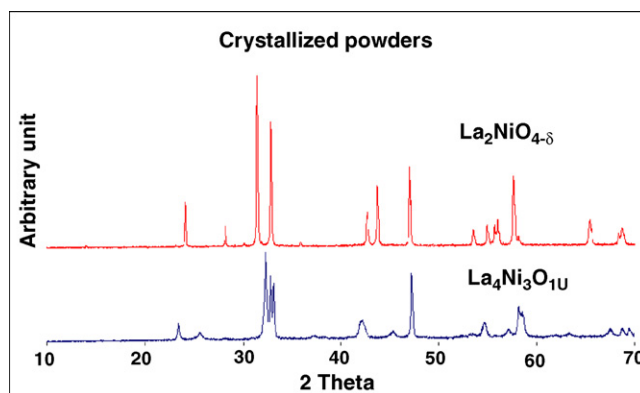


Fig. 3. X-ray diffraction patterns of powders.

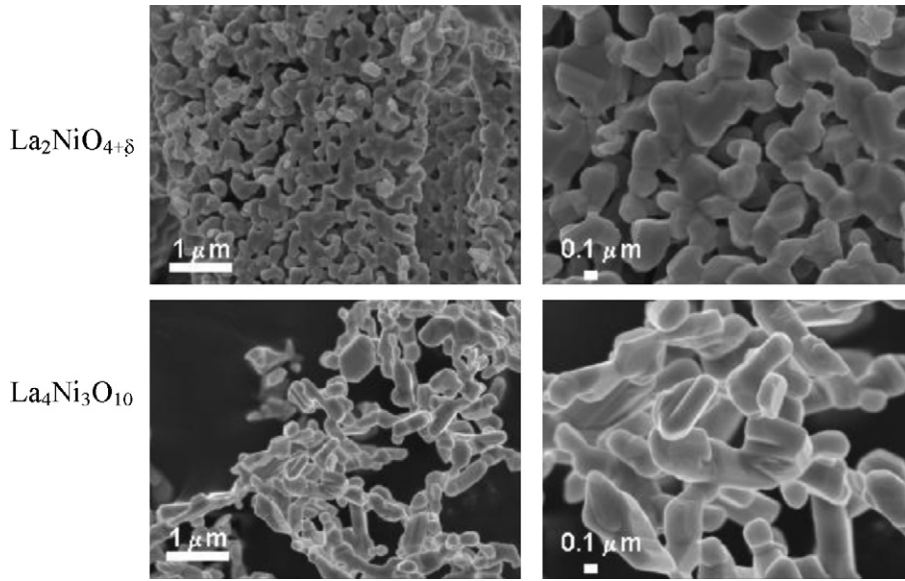


Fig. 4. SEM micrographs of $\text{La}_2\text{NiO}_{4+\delta}$ and $\text{La}_4\text{Ni}_3\text{O}_{10}$.

XRD pattern using Williamson and Hall diagram obtained by peak diffraction modelisation. Both powders calcined at $1000\text{ }^\circ\text{C}$ in air for 2 h (Fig. 3) have a crystallite size of about 280 nm for $\text{La}_2\text{NiO}_{4+\delta}$, while discrepancies in the 3D dimensions were found for $\text{La}_4\text{Ni}_3\text{O}_{10}$ leading to a crystallite size of about $150\text{ nm} \perp$ to c_{axis} and $550\text{ nm} \parallel c_{\text{axis}}$.

$\text{La}_2\text{NiO}_{4+\delta}$ powder has spherical grains shape (Fig. 4). The mean grain size determined from SEM micrograph was approximately 250–280 nm. These values are in good agreement with the crystallite size determined from XRD analysis, indicating that the grains are monocrystalline. $\text{La}_4\text{Ni}_3\text{O}_{10}$ particles are platelet shaped grains with dimensions of about 200 nm long and 600 nm large; these values are also in good agreement with those determined from XRD analysis, allowing similar conclusion than for $\text{La}_2\text{NiO}_{4+\delta}$ to be drawn.

Preliminary granulometry measurements performed on diluted suspensions made of powder dispersed in solvent, indicated a mean particle size of 1000 nm and 385 nm for $\text{La}_2\text{NiO}_{4+\delta}$ and $\text{La}_4\text{Ni}_3\text{O}_{10}$, respectively. Considering our previous results, one may thus conclude that $\text{La}_2\text{NiO}_{4+\delta}$ particles were more aggregated in suspension than $\text{La}_4\text{Ni}_3\text{O}_{10}$.

In order to improve the dispersion state of powders and to optimize the stabilization of the suspensions, an increasing amount of dispersant ratio (2, 4, 6 wt.% of powder) was added in the suspensions, as detailed in Table 1. Suspensions granulometry and Zeta potential measurements are reported in Fig. 5. Accordingly, the best dispersant concentration which corresponds to smaller aggregates and negative surface charge of particles, is 4% for $\text{La}_2\text{NiO}_{4+\delta}$,

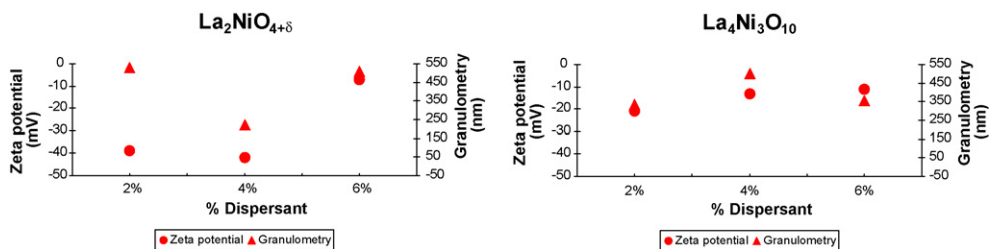


Fig. 5. Granulometry and Zeta potential measurements performed on powders dispersed in suspensions prepared with different amounts of dispersant.

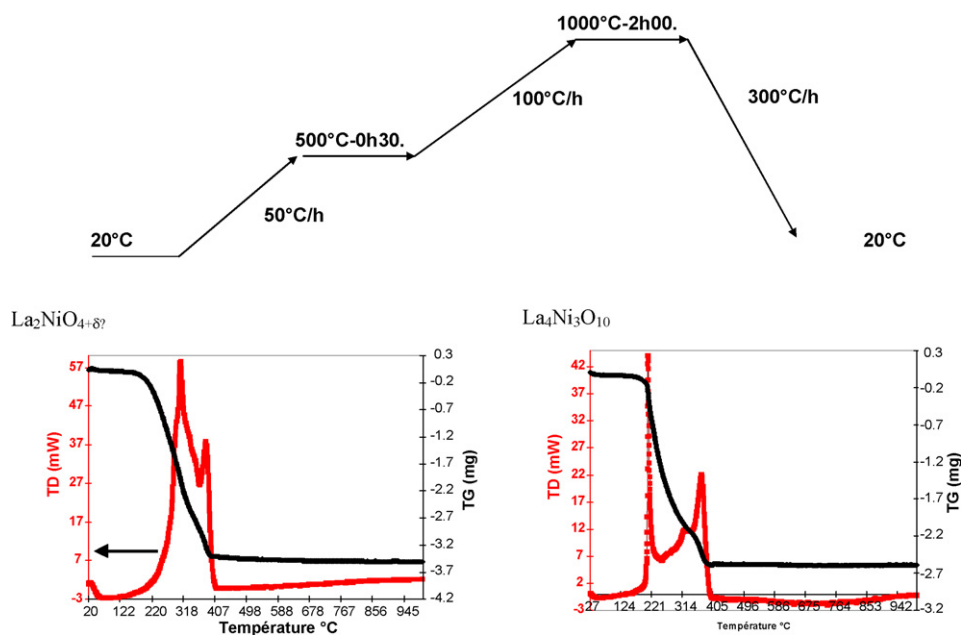


Fig. 6. Layer thermal profile and TG-TD curves.

and 2% for $\text{La}_4\text{Ni}_3\text{O}_{10}$. It is also worthwhile to notice that, for these ratio, the mean aggregate size of both oxides (about 250 nm for La_2NiO_4 and 350 nm for $\text{La}_4\text{Ni}_3\text{O}_{10}$) is in good agreement with the values determined from SEM and XRD analyses on powders. Thus, this shows that both powders were successfully dispersed in the suspensions while using an optimal amount of dispersant.

Suspensions decomposition in air was followed up by thermogravimetric (TG) and thermodifferential (TD) analyses as a function of increasing temperature in order to determine a suitable treatment for the annealing of $\text{La}_2\text{NiO}_{4+\delta}$ and $\text{La}_4\text{Ni}_3\text{O}_{10}$ films (Fig. 6). Accordingly, the decomposition of both suspensions is exothermic with critical step occurring in between 200 °C and 400 °C. Above this temperature, no more signal is observed. On this basis, an appropriate thermal profile was defined for the films annealing, as described in Fig. 6. A low heating rate was used below 500 °C during the burnout of organics in order to avoid cracks formation in films.

Surface and cross section micrographs of the different architectures I to IV are shown in Fig. 7. Their thickness is reported in Table 2. Accordingly, the multilayers are homogeneous, crack-free and adherent to the YSZ substrate.

The average thickness after three layer depositions is about 3.5 μm . As expected from the peculiar morphology of $\text{La}_2\text{NiO}_{4+\delta}$ and $\text{La}_4\text{Ni}_3\text{O}_{10}$ grains, thick films exhibit different microstructures depending on the selected architecture. The deposit of ceramic suspensions and the subsequent annealing of the films did not alter the shape of the grains. Indeed, Fig. 7 evidences the spherical and platelet shapes of $\text{La}_2\text{NiO}_{4+\delta}$ and $\text{La}_4\text{Ni}_3\text{O}_{10}$ grains in the electrodes (architectures I and II, respectively). Architectures III and IV made by combining $\text{La}_2\text{NiO}_{4+\delta}$ and

Table 2
Architectures Characteristics

Architecture	Thickness for 3 layers ($\pm 0.2 \mu\text{m}$)
I	4.1 μm
II	3.6 μm
III	3.8 μm
IV	3.3 μm

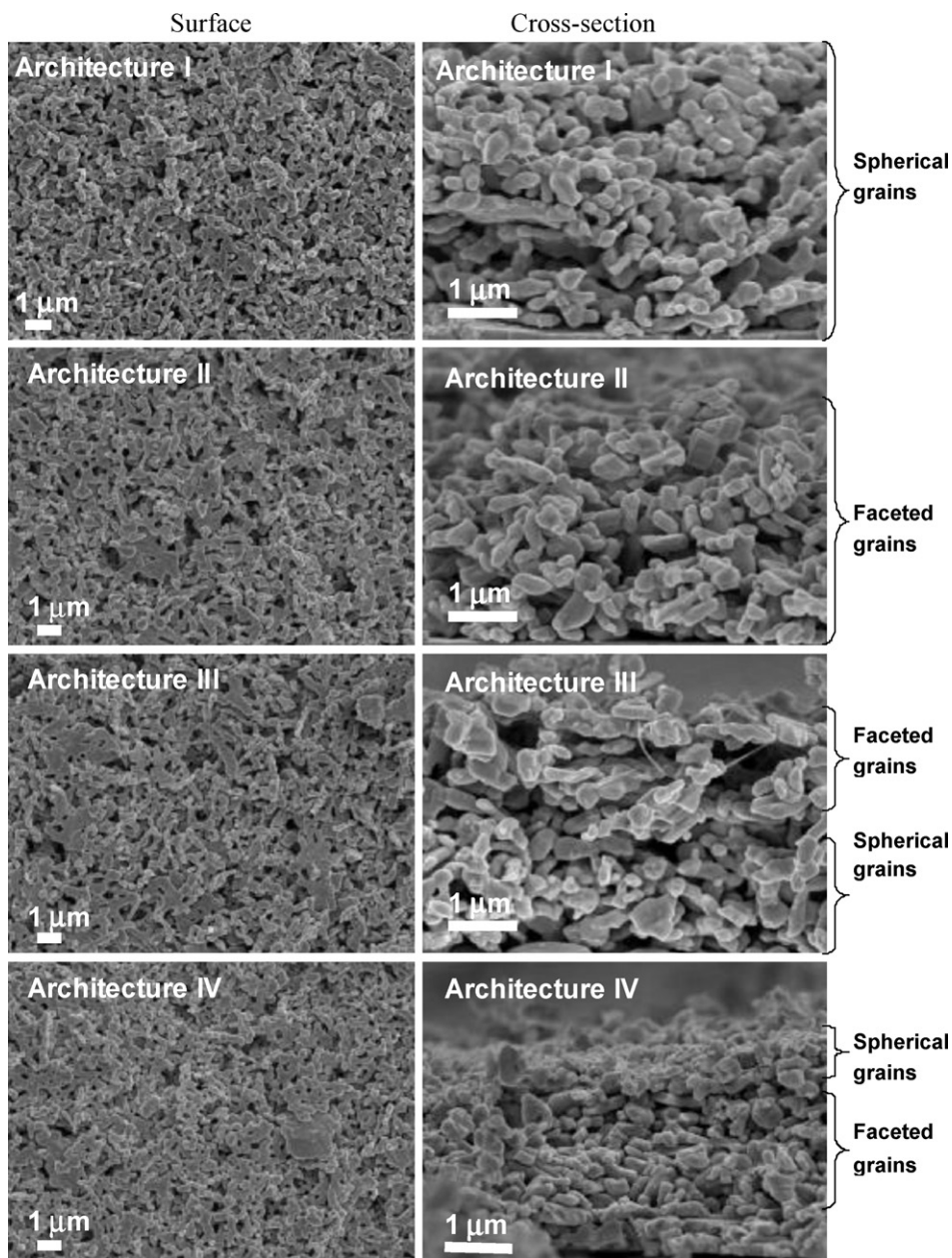


Fig. 7. SEM micrographs of architectures I to IV.

$\text{La}_4\text{Ni}_3\text{O}_{10}$ layers exhibit both peculiar shapes with grains disposed in accordance with the stacking of the different layers (see Fig. 2).

The porosity of these architectures consists of small pores of few hundred nanometers homogeneously distributed within the electrodes. Work is currently in progress for quantitative analysis of the porosity.

Cross section micrograph of architecture V is shown in Fig. 8. It can be seen that the thick cathodic layers are well adherent to the thin interlayer and exhibit a distinct microstructure, allowing us to define a “duplex microstructure” architecture for this cathode. The thin interlayer of nanoscale dimension exhibits an intimate contact interface with YSZ substrate, which is expected to reduce polarisation resistance by increasing the number of contact points at the cathode/electrolyte interface.

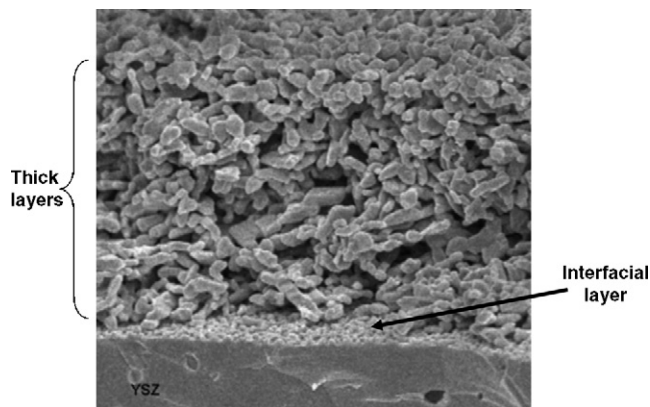


Fig. 8. SEM micrograph of architecture V.

4. Conclusion

We synthesized $\text{La}_2\text{NiO}_{4+\delta}$ and $\text{La}_4\text{Ni}_3\text{O}_{10}$ oxides via a sol-gel route and the X-ray powder diffraction analysis revealed single phases without impurities for both oxides. Both powders were shown to exhibit different morphologies (shape and size of grains). These lanthanum nickelates powders were mixed in an organic solvent using different dispersant ratio and additives to prepare stable slurries. An optimum concentration of dispersant was determined by means of several relevant characterization techniques. The stable slurries were used to dip-coat graded or monophase multilayered cathodes. After annealing, homogeneous, adherent and crack-free cathodes were obtained, exhibiting different microstructures in accordance with the peculiar morphology of the raw powders and the stacking of the layers. Duplex microstructure electrodes were designed by combining sol-gel route and slurry deposition technique. A thin interlayer of nanoscale dimension was coated onto the YSZ electrolyte in order to achieve intimate contact between the electrolyte and the cathode, and thick micro-scaled layers of tailored microstructure were added to increase the amount of active surface materials. The average thickness of the cathodes in this work was in the range of 3–4 μm .

References

- [1] E. Boehm, J.M. Bassat, P. Dordor, F. Mauvy, J.C. Grenier, Ph Stevens, *Solid State Sci.* 5 (2003) 973–981.
- [2] J.M. Bassat, P. Odier, A. Villesuzanne, C. Marin, M. Pouchard, *Solid State Ionics* 167 (2004) 341–347.
- [3] M.L. Fontaine, C. Laberty-Robert, A. Barnabé, F. Ansart, P. Tailhades, *Ceram. Int.* 30 (2004) 2087–2098.
- [4] M.L. Fontaine, PhD thesis (2004) Paul Sabatier University Toulouse III, France.
- [5] M.L. Fontaine, C. Laberty-Robert, F. Ansart, P. Tailhades, *J. Power Sources* 156 (1) (2006) 33–38.
- [6] M. Kleitz, F. Petitbon, *Solid State Ionics* 92 (1996) 65–74.
- [7] R. Moreno, *Am. Ceram. Soc. Bull.* 71 (10) (1992) 1521–1531.
- [8] R. Moreno, *Am. Ceram. Soc. Bull.* 71 (11) (1992) 1647–1657.
- [9] Z. Zhang, M. Greenblatt, *J. solid state chem.* 117 (1995) 236–246.
- [10] M. Greenblatt, Z. Zhang, M.H. Whangbo, *Synth. Met.* 85 (1997) 1451–1452.
- [11] T. Chartier, D. Merle, J.L. Besson, *J. Eur. Ceram. Soc.* 15 (1995) 101–107.
- [12] A. Navarro, J.R. Alcock, R.W. Whatmore, *J. Eur. Ceram. Soc.* 24 (2004) 1073–1076.
- [13] M.W. Murphy, T.R. Armstrong, P.A. Smith, *J. Am. Ceram. Soc.* 80 (1) (1997) 165–170.
- [14] E. Ivers-Tiffée, A. Weber, D. Herbstritt, *J. Eur. Ceram. Soc.* 21 (2001) 1805–1811.